Intensity Dependence of the Back Reaction and Transport of Electrons in Dye-Sensitized Nanocrystalline TiO_2 Solar Cells

A. C. Fisher,[†] L. M. Peter,*[,†] E. A. Ponomarev,[‡] A. B. Walker,[§] and K. G. U. Wijayantha[†]

Department of Chemistry, University of Bath, Claverton Down, Bath BA2 7AY, U.K., Department of Chemistry and Physics, University of Toronto, 80 St. George Street, Toronto, Ontario M5S 3H6, Canada, and Department of Physics, University of Bath, Claverton Down, Bath BA2 7AY, U.K.

Received: September 10, 1999; In Final Form: November 20, 1999

The lifetime τ_n and diffusion coefficient D_n of photoinjected electrons have been measured in a dye-sensitized nanocrystalline TiO_2 solar cell over 5 orders of magnitude of illumination intensity using intensity-modulated photovoltage and photocurrent spectroscopies. τ_n was found to be inversely proportional to the square root of the steady-state light intensity, I_0, whereas D_n varied with $I_0^{0.68}$. The intensity dependence of τ_n is interpreted as evidence that the back reaction of electrons with I_3^- may be second order in electron density. The intensity dependence of D_n is attributed to an exponential trap density distribution of the form $N_t(E) \propto \exp[-\beta(E - E_c)/(k_BT)]$ with $\beta \approx 0.6$. Since τ_n and D_n vary with intensity in opposite senses, the calculated electron diffusion length $L_n = (D_n\tau_n)^{1/2}$ falls by less than a factor of 5 when the intensity is reduced by 5 orders of magnitude. The incident photon to current efficiency (IPCE) is predicted to decrease by less than 10% over the same range of illumination intensity, and the experimental results confirm this prediction.

Introduction

Dye-sensitized nanocrystalline TiO_2 cells (DSNC) offer an alternative strategy for fabrication of low-cost thin film solar cells.[1−3] The chemical and physical processes involved in the operation of these cells take place in a two-phase system consisting of a porous nanocrystalline TiO_2 matrix interpenetrated by I_3^-/I^- redox electrolyte. Charge injection from the photoexcited adsorbed dye and regeneration of the dye by electron transfer from I^- lead to transport of electrons in the TiO_2 and of I_3^- and I^- ions in the electrolyte. Electron transfer from I^- to the oxidized dye and regeneration of I^- from I_3^- at the counter electrode link the two transport processes.

Not all of the injected electrons reach the back contact; some may react instead with I_3^-, reducing the incident photon-to-current conversion efficiency (IPCE). It has been shown that electron collection under short-circuit conditions occurs by diffusion.[4−7] The very low values of the diffusion coefficient ($<10^{-4}$ cm^2 s^{-1}) indicate that electron transport is determined by trapping and release of carriers from defect states at the surface or in the bulk of the nanocrystalline TiO_2. Electron transport and back reaction can be described in terms of the electron diffusion length $L_n = (D_n\tau_n)^{1/2}$, where D_n is the electron diffusion coefficient and τ_n is the electron lifetime. Both D_n and τ_n are known to depend on illumination intensity.[5,6] This raises the question of whether the intensity dependence of D_n and τ_n will result in an intensity-dependent IPCE. We have addressed this question by measuring D_n and τ_n over a wide range of illumination intensities. The experimental values of D_n and τ_n were used to calculate the IPCE from models of generation/collection/back reaction that includes either first- or second-order back reaction kinetics. Calculations predict that the IPCE should depend only weakly on light intensity. The satisfactory agreement between the calculated and measured IPCE values confirms the validity of the approach.

Theory

Factors Affecting the IPCE. The IPCE is determined by the product of the fraction of the incident light absorbed by the dye (f), the net electron injection efficiency (η), and the collection efficiency (H):

$$\mathrm{IPCE} = f\eta H \tag{1}$$

If radiative and nonradiative intramolecular decay of the excited state of the dye is much slower than electron injection, the net injection efficiency η is determined by the competition between regeneration of the dye by electron transfer from I^- to D^+ and recombination of electrons with D^+. The dye regeneration reaction is complicated by the fact that the overall reaction of iodide to triiodide involves the transfer of two electrons. The experimental evidence indicates that $I_2^{\bullet-}$ is formed in the first step.[8,9] A possible reaction sequence is as follows:

$$D^* \rightarrow D^+ + e_{cb} \quad \text{electron injection} \tag{2a}$$

$$D^+ + I^- \rightarrow D + I^\bullet \quad \text{dye regeneration} \tag{2b}$$

$$I^\bullet + I^- \rightarrow I_2^{\bullet-} \quad \text{formation of } I_2^{\bullet-} \tag{2c}$$

$$2I_2^{\bullet-} \rightarrow I_3^- + I^- \quad \text{disproportionation of } I_2^{\bullet-} \tag{2d}$$

$$D^+ + e_{cb} \rightarrow D \quad D^+/\text{electron recombination} \tag{2e}$$

Step 2e in this scheme can represent geminate recombination; i.e., the injected electron is still located in the conduction band of the TiO_2 particle to which D^+ is attached, and it returns to D^+ before being trapped. Alternatively, reaction 2e may involve

* To whom correspondence should be addressed. Phone/fax: +44 (0)-1225 826815. E-mail: l.m.peter@bath.ac.uk.
[†] Department of Chemistry, University of Bath.
[‡] Department of Chemistry and Physics, University of Toronto.
[§] Department of Physics, University of Bath.

10.1021/jp993220b CCC: $19.00
Published on Web 01/14/2000

any of a larger number of electrons already present in the particle. The second process becomes important at high intensities under open-circuit conditions where stationary electron densities in excess of 10^{17} cm^{-3} are expected (corresponding to more than one electron in each nanoparticle[10−12]). In either case, reaction 2e affects the net electron injection efficiency appearing in eq 1. The reaction scheme does not distinguish between free and trapped electrons, but in principle electrons trapped at surface sites may be involved in interfacial electron transfer. By contrast, electrons trapped in the bulk can only react after thermal detrapping.

The electron collection efficiency H is determined by the competition between collection of photoinjected electrons and their back reaction with I_3^- (also in principle with $I_2^{\bullet-}$). The reduction of I_3^- is not a simple one-step electron-transfer process. At platinum electrodes, dissociative chemisorption of I_2 allows facile electron transfer to $I_{ads}^{\bullet}$. At fluorine-doped SnO_2, by contrast, the electron-transfer rate constant determined by electrochemical impedance spectroscopy is over 10^5 times slower,[13] indicating that the iodine atom intermediate is not stabilized by chemisorption. This large difference in rate constants of the I_3^-/I^- reaction at platinum and at TiO_2/SnO_2 is essential for power generation in the DSNC. When the DSNC is illuminated, the I_3^-/I^- reaction remains close to equilibrium at the platinum electrode but is displaced far from equilibrium at the TiO_2 and SnO_2 surfaces, allowing the electrochemical potential of electrons in the TiO_2 (equivalent to qU_{photo}, where U_{photo} is the open-circuit potential) to increase by up to 0.8 eV.

Kinetics of the Back Reaction of Electrons with I_3^-. A possible back reaction sequence involving $I_2^{\bullet-}$ as an intermediate is[14−16]

$$I_3^- \rightleftharpoons I_2 + I^- \qquad K_1 \approx 10^{-7} \text{ mol dm}^{-3} \text{ in acetonitrile}^{17} \tag{3a}$$

$$I_2 + e \rightleftharpoons I_2^{\bullet-} \qquad K_2 \tag{3b}$$

$$2I_2^{\bullet-} \xrightarrow{k_{disp}} I_3^- + I^- \tag{3c}$$

$$I_2^{\bullet-} + e \xrightarrow{k_{et}} 2I^- \tag{3d}$$

In this scheme, the disproportionation reaction 3c competes with the direct electron transfer (reaction 3d). If reaction 3b is in equilibrium, as proposed by Huang et al.,[14] and if reaction 3d is neglected, the rate of decay of electron density will be given by

$$\frac{dn}{dt} = -k_{disp}K_1^2K_2^2\frac{[I_3^-]^2n^2}{[I^-]^2} \tag{4}$$

(This would be consistent with the observation that $dn/dt \propto n^{2.2}$ reported by Schlichthörl et al.[16]). If, on the other hand, reaction 3d is the predominant route, the rate of decay of electron density is given by

$$\frac{dn}{dt} = -2k_{et}K_1K_2\frac{[I_3^-]n^2}{[I^-]} \tag{5}$$

Note that in both cases, the decay of electron density is second order in n. In this case, the electron lifetime can be defined for small-amplitude perturbations of n as

$$\tau_n = \frac{1}{kn} \tag{6a}$$

where

$$k = k_{disp}K_1^2K_2^2\frac{[I_3^-]^2}{[I^-]^2} \tag{6b}$$

or

$$k = 2k_{et}K_1K_2\frac{[I_3^-]}{[I^-]} \tag{6c}$$

depending on whether reaction 3c or 3d predominates. The steady-state excess electron density at open circuit is given in either case by $n = (G/k)^{1/2} = G\tau_n$, where G is the net rate of electron injection (cm^3 s^{-1}). It follows that the electron lifetime in the small-amplitude limit is given by $\tau_n = (Gk)^{-1/2}$; i.e., it is inversely proportional to the square root of the light intensity if η is constant. It is important to note that eqs 6a−6c show that the determination of reaction orders with respect to $[I_3^-]$ and $[I^-]$ from small-amplitude intensity-modulated photovoltage spectroscopy (IMVS) measurements must be made at constant steady-state electron density (n), not at constant illumination intensity.

In both of the preceding mechanisms, the rate of decay of electrons is second order in electron density. This contrasts with the kinetics of the alternative pathway involving dissociative chemisorption of I_2:

$$I_3^- \rightleftharpoons I_2 + I^- \qquad K_1 \tag{7a}$$

$$I_2 \rightleftharpoons 2I^{\bullet} \qquad K_3 \tag{7b}$$

$$I^{\bullet} + e \rightarrow I^- \qquad k_a \tag{7c}$$

In this case the decay of electron density is first order in electron density,

$$\frac{dn}{dt} = -k_a n\sqrt{\frac{K_1K_3[I_3^-]}{[I^-]}} \tag{8}$$

The pseudo-first-order electron lifetime τ_n can therefore be defined as

$$\tau_n = \frac{1}{k_a\sqrt{\dfrac{K_1K_3[I_3^-]}{[I^-]}}} \tag{9}$$

Note that in this case the electron lifetime is independent of the net electron injection rate G.

Electron Transport. Electrons are collected at the substrate electrode (F-doped SnO_2). The contribution of electric fields to electron transport in the bulk of the TiO_2 layer is generally considered to be negligible[7,18] so that electrons reach the back contact by diffusion. However, electron diffusion in nanocrystalline TiO_2 is remarkably slow, and it appears to be dominated by trapping/detrapping processes. The apparent electron diffusion coefficient D_n determined by intensity-modulated photocurrent spectroscopy (IMPS) is intensity-dependent.[5,6] At solar illumination levels, D_n is typically 5×10^{-5} cm^2 s^{-1},[6] which is more than 2 orders of magnitude smaller that the value for bulk anatase.[19] It is therefore reasonable to suppose that the majority of electrons are trapped and that the trapping/detrapping processes determine the effective diffusion coefficient. The upper limit of the diffusion coefficient should correspond to

the movement of free electrons in the conduction band. The electron mobility in the nanocrystalline phase may be lower than in the bulk oxide as a consequence of solvent polarization effects, but as shown below, there is no experimental evidence that the diffusion coefficient approaches an upper limit; i.e. it is determined by trapping rather than polarization effects.

If a large-amplitude light pulse is used to perturb the system from an initial dark equilibrium condition, electron transport in the nanocrystalline phase will be influenced by the wide range of residence times of electrons in traps. Under these nonstationary conditions, the concept of effective diffusion coefficient is not useful, and the electron transport is best described in terms of a distribution of residence times.[20,21] Nevertheless, D_n can be regarded as an intensity-dependent quantity in the case where a small-amplitude periodic perturbation of the illumination is superimposed on a much larger steady-state illumination level that determines the position of ${}_nE_F$, the electron quasi Fermi level (QFL) (Figure 2 below). It can be shown that the apparent diffusion coefficient for electrons is determined by the density of trapping states located at the QFL.[22,23] This allows definition and measurement of D_n for a particular illumination level. If the first-order rate constants for trapping (k_t) and detrapping (k_d) are large compared with the measurement frequency, the IMPS response is expected to have the same shape as in the absence of trapping. The only change is that the frequency response is determined by the effective diffusion coefficient $D_n = D_{cb}(k_d/k_t)$, where D_{cb} is the diffusion coefficient of electrons in the conduction band. D_n is found to be more than 2 orders of magnitude lower than D_{cb} even at 1 sun, indicating that k_d/k_t is small, even at high light intensities (see Appendix for details). D_n is expected to vary with light intensity as ${}_nE_F$ moves through a distribution of trapping levels, since k_d depends exponentially on $(E_c - {}_nE_F)$ and k_t depends on the density of vacant trapping states at $E = {}_nE_F$.

Steady-State Electron Concentration Profiles. If the TiO_2/electrolyte system is treated as a quasi-homogeneous nonscattering medium and the perturbation of electrolyte composition is neglected, the generation and collection of electrons in the DSNC can be described by the continuity equation[4,7]

$$\frac{\partial n}{\partial t} = \eta\alpha I_0 \, e^{-\alpha x} + D_n \frac{\partial^2 n}{\partial x^2} - \frac{n - n_0}{\tau_n} \qquad (10)$$

Here, I_0 is the incident photon flux corrected for reflection losses, $\alpha(\lambda)$ is the wavelength-dependent absorption coefficient (determined by the dye coverage), n is the density of electrons under illumination, and n_0 is the equilibrium electron density in the dark.

The last term in eq 10 describes the pseudo-first-order decay of electrons by reaction with I_3^-. However, if the decay of electrons is second order in n (eqs 4 and 5), eq 10 should be rewritten as

$$\frac{\partial n}{\partial t} = \eta\alpha I_0 \, e^{-\alpha x} + D_n \frac{\partial^2 n}{\partial x^2} - k(n - n_0)^2 \qquad (11)$$

where k is defined by eq 6b or 6c.

Two boundary conditions are required for the general solutions of eqs 10 and 11. The first is that the gradient of electron density is zero at $x = d$ (electrolyte side). The second is that the flux of electrons at $x = 0$ is equal to the rate of their extraction, i.e., $D_n(\partial n/\partial x)_{x=0} = k_{ext}(n - n_0)$, where k_{ext} is the rate constant for electron extraction at the substrate.[6] General solutions for the small-amplitude modulated response are given in the Appendix. The solution for the diffusion-limited short-circuit case is obtained by allowing k_{ext} to become large, whereas the open-circuit case is obtained by setting $k_{ext} = 0$. Note that the electron density increases linearly with intensity in the case where the back reaction of electrons with triiodide is first order in n, whereas it increases with the square root of the intensity if the reaction is second order in n. In the first-order case, τ_n is expected to be independent of intensity, whereas in the second-order case, τ_n (in the linearized small-amplitude limit) is proportional to $1/n$ and hence to $I_0^{-0.5}$.

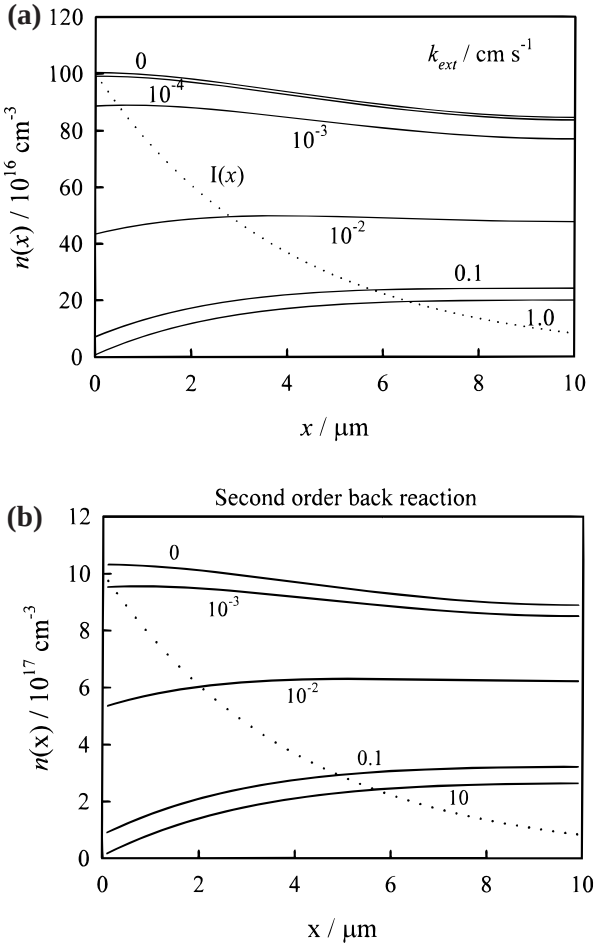

Figure 1. Electron density profiles calculated for a range of k_{ext} values between the limits of open circuit ($k_{ext} = 0$) and closed circuit (large k_{ext}) with $I_0 = 10^{16}$ cm^2 s^{-1}, $\alpha = 2500$ cm^{-1}, $D_n = 10^{-5}$ cm^2 s^{-1}, $d = 10$ μm, k_{ext}/cm s^{-1} as shown on the plots: (a) first-order back reaction of electrons with I_3^-, $\tau_n = 0.1$ s; (b) second-order back reaction of electrons with I_3^-, $k_2 = 10^{-17}$ cm^{-3} s^{-1}. Illumination is from the substrate side (intensity profile shown as dotted line).

Figure 1 shows steady-state electron density profiles calculated for the first- and second-order cases between the limiting cases corresponding to open circuit ($k_{ext} = 0$) and short circuit (k_{ext} large). To aid comparison, the first- and second-order rate constants for the back reaction of electrons with I_3^- have been chosen to correspond to the same small-amplitude electron lifetime (eqs 6b and 6c). The values of absorption coefficient, film thickness, and D_n used in the calculations are typical for practical DSNCs.

The electrochemical potential of electrons in the nanocrystalline TiO_2 corresponds to the electron QFL, ${}_nE_F$, which is defined by the expression

$$\frac{n_0 + \Delta n}{n_0} = e^{-(nE_F - E_F)/(k_B T)} \approx \frac{\Delta n}{n_0} \qquad (12)$$

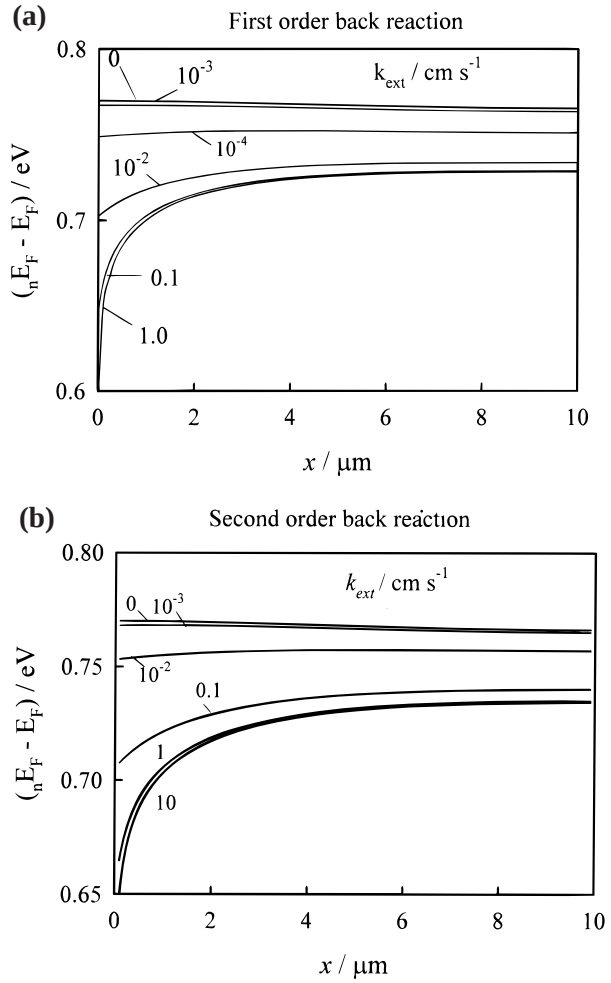

Figure 2. QFLs calculated from electron density profiles in Figure 1: (a) first-order back reaction of electrons; (b) second-order back reaction of electrons with I_3^-. Equilibrium electron density in the dark (n_0) is 10^5 cm^{-3}. Values of k_{ext} are as shown.

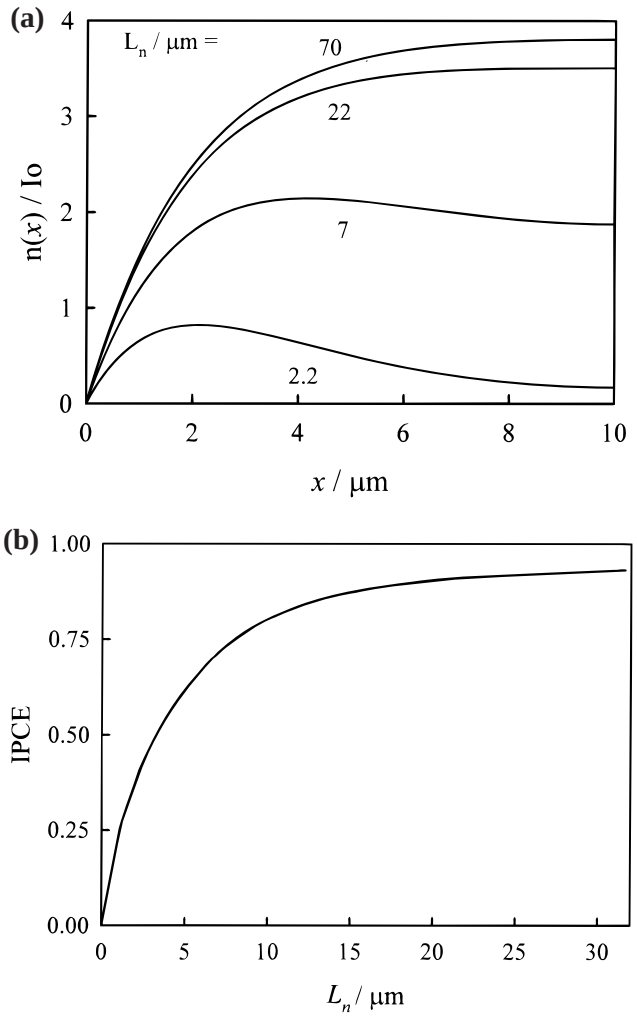

Figure 3. Influence of L_n on steady-state electron density profiles and IPCE, calculated for first-order back reaction, with $d = 10$ μm, $a = 3000$ cm^{-1}: (a) normalized electron density profiles at short circuit; (b) IPCE as a function of the electron diffusion length.

Here, $\Delta n = (n - n_0)$ is the excess electron density in the conduction band, which can be assumed to be much greater than the equilibrium (dark) value n_0 for all intensities of practical interest. E_F is the equilibrium Fermi level (determined by the I^-/I_3^- redox couple). The position of the electron QFL at $x = 0$ under illumination determines the photovoltage: $qU_{photo} = (_nE_F - E_F)$. For the calculations of the QFL profiles, n_0 was taken to be 10^5 cm^{-3} (based on the position of the I_3^-/I^- redox Fermi level relative to the conduction band of TiO_2). Figure 2 contrasts the QFLs for different rates of electron extraction ranging between the short-circuit and open-circuit limits. The plots show that the difference between the electron QFLs under open-circuit and short-circuit conditions is rather small except close to the contact.

In the context of this discussion of the electron QFLs, it is worth remarking that the potential difference between the center of the particles and the bulk of the solution is not perturbed significantly by the illumination. Band bending in the particles can be neglected, and elementary electrostatics shows that the photoinduced change in the potential drop across the Helmholtz layer will also be negligibly small at the light intensities used in this study (see also ref 24). The photovoltage measured in the external circuit arises from the fact that the Fermi energy of the contact rises as the QFL of electrons in the TiO_2 phase increases. This upward shift of $_nE_F$ in the substrate will, however, modify the potential drop at the SnO_2/TiO_2 interface, which has been calculated by Bisquert et al.[24] and by Schwarzburg and Willig.[25]

The steady-state electron concentration profiles calculated for open-circuit and short-circuit conditions as a function of the rate constant for the back reaction of electrons with I_3^- have been presented elsewhere.[26] Increasing the rate of back reaction (and hence reducing the diffusion length L_n) introduces a peak in the electron concentration profile as illustrated in Figure 3a, and electrons generated deeper in the film will diffuse from the substrate and be lost by back reaction with I_3^-. For illumination from the substrate side, the condition for efficient electron collection ($H \rightarrow 1$) can be expressed by the inequality $L_n > \alpha^{-1}$. Figure 3b shows how decreasing the electron diffusion length affects the IPCE of a typical DSNC.

Calculations for the open-circuit case[26] indicate that the excess electron density (and hence the electron QFL) can be considered to a first approximation as independent of distance, provided that the electron diffusion length is greater than the penetration depth of the light, $1/\alpha$. If this condition is not fulfilled, $_nE_F$ will be lower on the electrolyte side compared with the substrate side if the cell is illuminated from the substrate side. Reversal of the direction of illumination should reverse the electron density profile and lower the photovoltage. The effect is expected to be very small in experimental cells, which nearly always fulfill the condition $L_n > \alpha^{-1}$.

IMPS and IMVS. Equation 10 is based on the assumption that the decay of electrons is first order. However, it can still be used to derive the photovoltage and photocurrent response to small-amplitude perturbations for the case where the decay is second order in n (eq 11); the lifetime τ_n is then defined by eq 6a. Analytical solutions have been given previously[6] for small-amplitude sinusoidal perturbation of the incident light intensity of the form

$$I(t) = I_0[1 + \delta\, e^{i\omega t}] \qquad (13)$$

where $\delta \ll 1$. General solutions for illumination from the substrate side are given in the Appendix.

The periodic solution for open-circuit conditions is obtained in the limit $k_{ext} \rightarrow 0$. Under these conditions, relaxation of the electron density occurs entirely by back reaction with I_3^- so that the periodic photovoltage response is characterized by a time constant equal to τ_n (the change in electron QFL is linearly proportional to the modulation of n for small-amplitude perturbations). The intensity-modulated photovoltage spectroscopy (IMVS) response is a semicircle with a minimum occurring at the angular frequency $\omega_{min}(IMVS) = 2\pi f_{min} = \tau_n^{-1}$.[12,15] Solutions for the short-circuit case are obtained in the limit of large k_{ext} (Appendix). Further details can be found in refs 6 and 12.

If, as is the case for the DCNC, electron trapping (rate constant k_t, s^{-1}) and detrapping (rate constant k_d, s^{-1}) occur, it is necessary to consider the influence on the IMVS and IMPS response. This has been done previously[6] (see also Appendix). If $k_t \gg k_d$, it can be shown that ω_{min}(IMVS) is equal to the reciprocal of the lifetime of trapped electrons, τ_t. Under conditions where $k_t > k_d > \omega$, the effects of trapping/detrapping on the IMPS response lead to the definition of an effective diffusion coefficient $D_n = D_{cb}(k_d/k_t)$, where D_{cb} is the diffusion coefficient of electrons in the conduction band. If the IMPS plots fit the expressions for the trap-free case, but $D_n \ll D_{cb}$, it can be assumed that the condition $k_t \gg k_d > \omega$ is satisfied. In practice, the IMPS response in this limit is identical to that calculated for the trap-free case in ref 6 (Appendix) except that the diffusion coefficient is given by $D_n = D_{cb}(k_d/k_t)$. If τ_t, α, and d are known, D_n can be obtained by fitting ω_{min}(IMPS) using the analytical solution for the trapping case and varying the ratio k_t/k_d (Appendix). It is reasonable to assume that $\tau_{cb} > \tau_t$ in the fitting if the back reaction occurs via surface states. If most electrons are collected at the substrate ($H \rightarrow 1$), the fitting becomes insensitive to the lifetime of free and trapped electrons determined by back reaction (τ_{cb} and τ_t, respectively).

It follows from this discussion that τ_t and D_n can be determined as a function of dc illumination intensity by IMPS and IMVS, respectively. For simplicity, the values of τ_t and D_n obtained by fitting the experimental responses are denoted as τ_n and D_n in the figures and text.

Figure 1 shows that the steady-state component of the electron density is not identical in IMPS and IMVS experiments, even if the dc illumination intensity is the same. If the electron lifetime is inversely proportional to the steady-state electron density (second-order case, eq 6a), the use of the open-circuit value of τ_n in the calculation of $L_n = (D_n\tau_n)^{1/2}$ will result in underestimation of the electron diffusion length at short circuit.

Experimental Section

DSN cells were fabricated using sol−gel films prepared by the techniques developed by Nazeeruddin et al.[3] Conductive glass substrates (Libby Owens Ford, 10 Ω/square SnO_2) were cleaned by overnight immersion in a solution of KOH in 2-propanol, rinsed with deionized water, and dried in an air stream. The TiO_2 colloid was spread over the substrate with a glass rod using adhesive tape spacers. The plate was dried in air for a few minutes and then fired at 450 °C for 30 min in air, resulting in an almost transparent film. The active area of the cell was 1 cm^2, and the thickness of the TiO_2 layer determined by scanning electron microscopy was 6 μm. The film was immersed overnight in a 3×10^{-4} M solution of *cis*-di(thiocyanato)-*N*,*N*-bis(2,2′-dicarboxylate)ruthenium(II) (Solaronix) in dry ethanol for dye absorption. After dye absorption, the electrode was dried and stored under argon. A sandwich cell was prepared with a second conductive glass coated with sputter-deposited Pt, and both plates were sealed together with transparent polyethylene (PE) hot melt film. The electrolyte was introduced through holes drilled in the counter electrode, and these were sealed subsequently with microscope cover plates and PE hot melt. The electrolyte was composed of 0.85 M methylhexylimidazolium iodide (MHImI), 0.05 M iodine, 0.1 M LiI, and 0.2 M 4-*tert*-butylpyridine in acetonitrile. Analytical grade iodine (BDH), acetonitrile (Aldrich), and 4-*tert*-butylpyridine (Aldrich) were used without further purification. MHImI was kindly provided by the Institut fur Angewandte Photovoltaik, Gelsenkirchen. The transmission of the cells was measured using a SnO_2(F)-coated plate as reference, and the absorption coefficient was calculated from the film thickness. The IPCE measured at 10^{15} photons cm^{-2} s^{-1} was 0.79, which is in good agreement with the value of 0.78 calculated from $\alpha = 2500$ cm^{-1} and $d = 6$ μm, assuming $\eta = 1$.

IMVS and IMPS measurements were carried out using a blue-light-emitting diode ($\lambda_{max} = 470$ nm) driven by a Solartron 1250 frequency response analyzer. The LED provided both the dc and ac components of the illumination. The ac component of the current to the LED generated a small modulation superimposed on the dc light intensity. The intensity incident on the DSN cell was adjusted by insertion of calibrated neutral density filters (Schott NG3). The dc light intensity was measured using a calibrated silicon diode (traceable to NBS). Since measurements were made to very low light intensities, special precautions were needed to eliminate electrical noise. Measurements were performed in an earthed Faraday box, and computer equipment was shielded to prevent interference. Photocurrents were measured using a battery-operated potentiostat constructed using low-noise operational amplifiers. Photovoltages were measured using a high-impedance low-noise battery-operated preamplifier (Stanford SR560, input impedance of 10^8 Ω). The IMVS (open-circuit) and IMPS (short-circuit) responses were recorded over the appropriate frequency range using a Solartron 1250 frequency response analyzer under computer control.

Results and Discussion

Figure 4 shows typical experimental IMVS and IMPS plots for the DSNC. The shape of these plots has been discussed elsewhere.[6,7] The effects of *RC* attenuation[6,7] on the present set of IMPS results is negligible, so interpretation is straightforward. As shown previously,[6] the shape of the IMPS plots can be fitted satisfactorily using the IMPS solution for the trap-free case and an effective diffusion coefficient $D_n \ll D_{cb}$. This confirms that the condition $k_t > k_d > \omega$ is fulfilled. The main features of interest are the frequencies at which the minima in the IMVS and IMPS plots occur for a particular illumination intensity. The frequencies ω_{min}(IMVS) and ω_{min}(IMPS) were derived from the measured data using logarithmic interpolation.

Figure 5 illustrates the influence of the dc light intensity on the measured values of ω_{min}(IMVS) and ω_{min}(IMPS). It can be

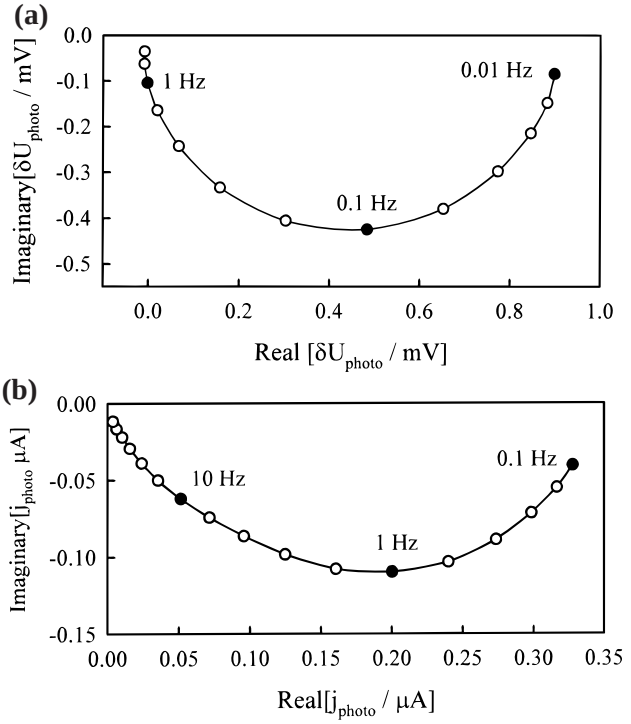

Figure 4. (a) Typical IMVS response. (b) Typical IMPS response of DSNC. $d = 6\ \mu$m, $\alpha = 2300\ \text{cm}^{-1}$, $I_0 = 4 \times 10^{13}\ \text{cm}^{-2}\ \text{s}^{-1}$, $\lambda = 470$ nm, IPCE = 0.75.

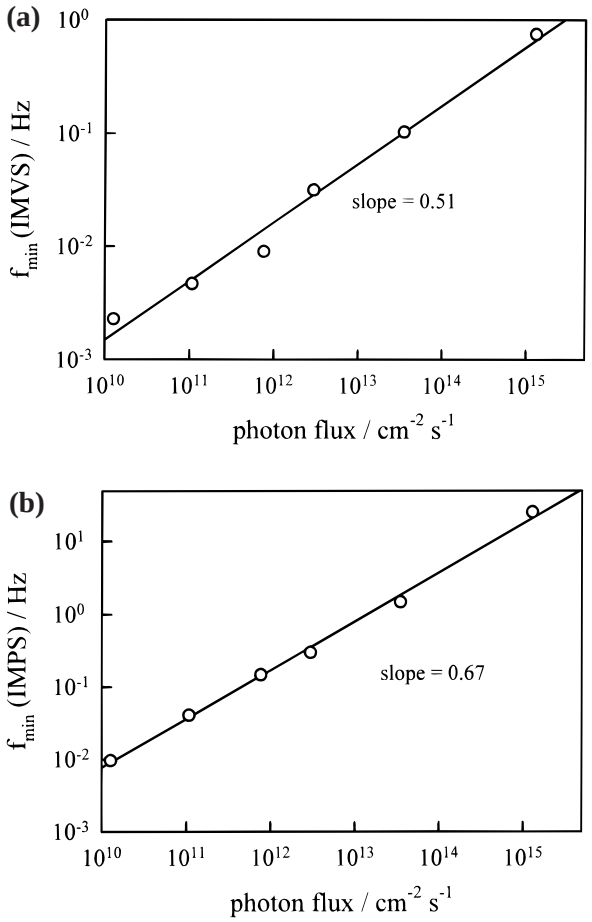

Figure 5. Log−log plots showing variation of (a) f_{min}(IMVS) and (b) variation of f_{min}(IMPS) with incident dc photon flux.

seen that both increase with light intensity. At the lowest light intensities (corresponding approximately to 10^{-6} sun), the IMVS and IMPS responses are extraordinarily slow, indicating a long electron lifetime and slow electron transport, respectively.

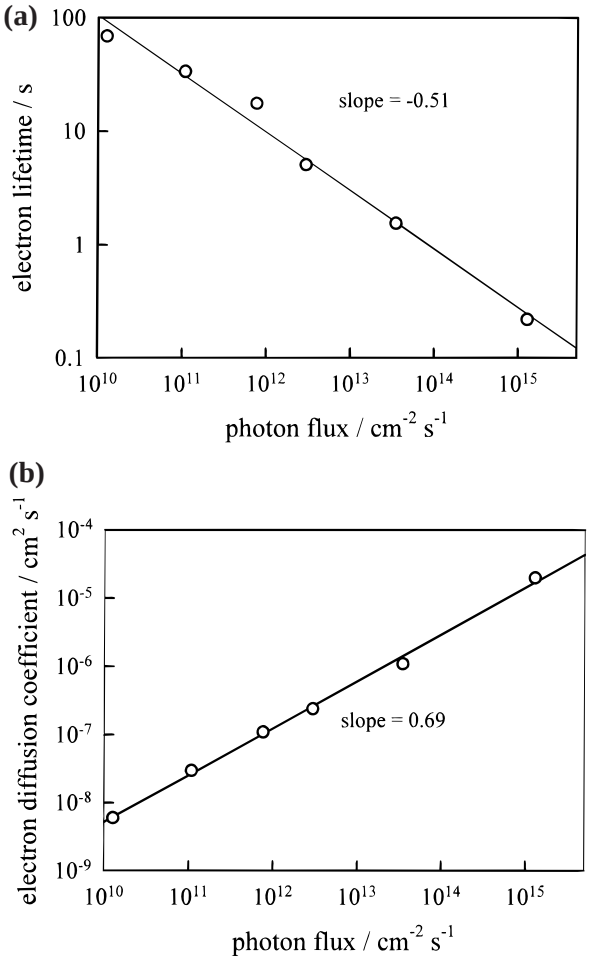

Figure 6. (a) Variation of electron lifetime τ_n under open-circuit conditions as a function of the incident dc photon flux. (b) Variation of effective electron diffusion coefficient D_n with incident dc photon flux. D_n is obtained by fitting the IMPS response as described in the text.

The intensity dependence of τ_n was derived directly from ω_{min}(IMVS). In principle, D_n can be obtained using the expressions for the trap-free case, since, as shown below, essentially all injected electrons are collected and the IMPS response becomes insensitive to the electron lifetime. A more rigorous approach involves considering the effects of trapping. The intensity dependence of D_n was derived from ω_{min}(IMPS) by curve-fitting using $\alpha = 2500\ \text{cm}^{-1}$, $d = 6\ \mu$m, and the τ_n ($=\tau_t$) value derived from IMVS at the same intensity. The expressions for the trapping/detrappping case (eq A5 in the Appendix) were used for the fitting. D_{cb} was taken as $10^{-2}\ \text{cm}^2\ \text{s}^{-1}$,[18] τ_t was taken from the IMVS data, and the ratio k_t/k_d was then varied to fit ω_{min}(IMPS). k_t was taken as $10^8\ \text{s}^{-1}$ to ensure that the condition $k_t > k_d > \omega$ was fulfilled. τ_{cb} was taken as 10 s. D_n was then obtained as $D_n = D_{cb}(k_d/k_t)$. It is important to note that the choice of D_{cb} does not affect the value of D_n obtained, provided that $k_t \gg k_d$, i.e., if most electrons are trapped. Similarly, the fitting is insensitive to τ_{cb} provided that it is not unreasonably small. As expected, the values of D_n obtained by this more rigorous approach were almost identical to those obtained using the expressions for the trap-free case in the limit of negligible back reaction.

The calculated variations of τ_n and D_n with incident photon flux are presented in Figure 6 as double-logarithmic plots. The

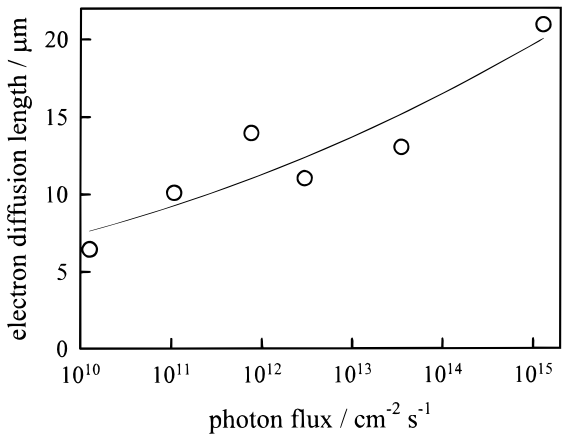

Figure 7. Variation of estimated electron diffusion length $L_n = (D_n\tau_n)^{1/2}$ with incident photon flux.

slopes of the τ_n and D_n plots are -0.51 and 0.68, respectively.

The electron diffusion length $L_n = (D_n\tau_n)^{1/2}$ was calculated as a function of light intensity using the values of τ_n and D_n derived from the IMVS and IMPS responses, respectively. Figure 7 shows that L_n is only weakly dependent on light intensity, varying by less than a factor of 5 over 5 orders of magnitude of illumination intensity. This is a consequence of the fact that D_n and τ_n vary in opposite senses. As pointed out in the theoretical section, L_n will be underestimated if the back reaction is second order in electrons, since the short-circuit lifetime will be longer than the open-circuit lifetime that appears in the expression for L_n. Estimates suggest that the true value of L_n in this case may be 2−3 times larger than the values shown in Figure 7.

The dependence of τ_n on light intensity is very close the square root dependence expected for the second-order mechanisms involving $I_2^{\bullet-}$ as an intermediate (eqs 3a−3d). The intensity dependence of τ_n has been noted previously by Schlichthörl et al.,[15,16] who attributed it to the variation of the electron-transfer rate with the energy level of trapped electrons. The same authors showed that a 5-fold increase in I_3^-/I^- concentration lowered τ_n by a factor of 25 (it is important to note that this comparison was made at constant open-circuit voltage, i.e., for constant n in eq 6a). This result shows that the reaction of electrons with I_3^- is second order in I_3^- concentration and corresponds to reactions 3a−3c. This contradicts the conclusions of Liu et al.[27] who reported that the reaction is first order in $[I_3^-]$ and proposed that the mechanism involves dissociative chemisorption of I_2 (eqs 7−9). Schlichthörl et al.[16] have recently reported that the rate of electron decay is proportional to $n^{2.2}$, which is consistent with the second-order mechanism. Further work is in progress to determine the reaction orders with respect to I_3^- and I^- using IMVS.

The formation of $I_2^{\bullet-}$ during the photooxidation of iodide at bare[28] and dye-covered[8] TiO_2 colloids is well established. The initial oxidation of I^- to I is followed by diffusion-controlled reaction with I^- to form $I_2^{\bullet-}$. The $I_2^{\bullet-}$ decays either by disproportionation or by back reaction with electrons in surface traps. Fitzmaurice and Frei[8] reported a value of 3×10^9 dm^3 s^{-1} for the rate constant for disproportionation of $I_2^{\bullet-}$ to I_3^-. This value is a rough guide only, since it was obtained in experiments using aqueous colloidal suspensions of TiO_2 sensitized with phenylfluorone. The formation constant for triiodide in acetonitrile is on the order of 10^7 mol dm^{-3},[17] so $K_1 = 10^{-7}$. An order of magnitude value of the second-order rate constant k (eq 6b) can be estimated from the measured lifetime, which is close to 1 s for an incident photon flux of 6×10^{13} cm^{-2} s^{-1}. Since $d = 6$ μm and 70% of the incident light is absorbed, the mean electron injection rate G is 7.3×10^{16} cm^{-3} s^{-1}. For the second-order case k is $1/(\tau_n^2 G)$, so the rate constant k is 1.4×10^{-17} cm^3 s^{-1}, or 8.4×10^3 dm^3 mol^{-1} s^{-1}. Using these values and inserting the appropriate concentrations of I_3^- and I^- in eq 6b gives $K_2 \approx 3 \times 10^5$ mol^{-1} dm^3, showing that the equilibrium reaction 3b favors $I_2^{\bullet-}$ as expected.

The intensity dependence of D_n reflects the change in the ratio of free to trapped electron densities as the QFL moves toward the conduction band with increasing intensity. The case of trapping/detrapping involving a single level has been considered previously;[6,12] the more realistic case of trapping/detrapping from a distribution of energy levels has been treated recently by Vanmaekelbergh and de Jongh,[22] but they neglect the back reaction. An alternative approach adopted by Nelson[21] is to use a continuous time random walk model to simulate electron transport in terms of a distribution of waiting times. Fitting of large-amplitude photocurrent transients by this approach was achieved using a trap distribution of the form $g(E) \propto \exp[(\beta(E_c - E)/(kT)]$ with $\beta = 0.37$.

Details of an extension to the approach of Vanmaekelbergh and de Jongh will be given elsewhere.[23] Here, a brief summary of the approach suffices to rationalize the experimental results. If k_t/k_d, the ratio of the first-order rate constants for trapping and detrapping, is much larger than unity, the effective diffusion coefficient is given by (see Appendix)

$$D_n = D_{cb}\left(\frac{k_d}{k_t}\right) \tag{14}$$

where D_{cb} is the diffusion coefficient of free electrons. Since D_{cb} is on the order of 10^{-2} cm^2 s^{-1} for bulk anatase,[19] it is clear from the measured values of D_n that the ratio k_d/k_t lies in the range $10^{-3}-10^{-6}$. For traps located at a single energy, $k_t = \upsilon_{th}\sigma_t(1 - f_T)N_t$, where N_t is the volume trap density, υ_{th} is the thermal velocity of electrons in the conduction band, and σ_t is the capture cross section of the traps. k_d, on the other hand, depends linearly on the density of filled traps $f_T N_t$ and exponentially on the trap depth $E_c - E_T$. Here, f_T is the Fermi Dirac function defined for $E = E_T$:

$$f_T = \frac{1}{1 + \exp\left[\dfrac{E - E_T}{k_B T}\right]} \tag{15}$$

For a distribution of traps, the ratio k_d/k_t is obtained by integrating the trapping and detrapping rates over the energy range from E_v to E_c. The integrals contain the weighting function

$$g(E - {}_nE_F) = f(E - {}_nE_F)\,[1 - f(E - {}_nE_F)] \tag{16}$$

which peaks sharply at $E = {}_nE_F$, where $g = {}^1/_4$. The trapping/detrapping behavior is therefore dominated by the density of occupied and vacant traps over a narrow energy range located at $E = {}_nE_F$, and g can be approximated by the δ function $k_B T\,\delta(E_T - {}_nE_F)$.

An exponential density of states distribution of traps is usually described by the expression[20]

$$s(E_T) = \frac{N_{T0}}{k_B T_T}\exp\left[\frac{-(E_c - E_T)}{k_B T}\right] \tag{17a}$$

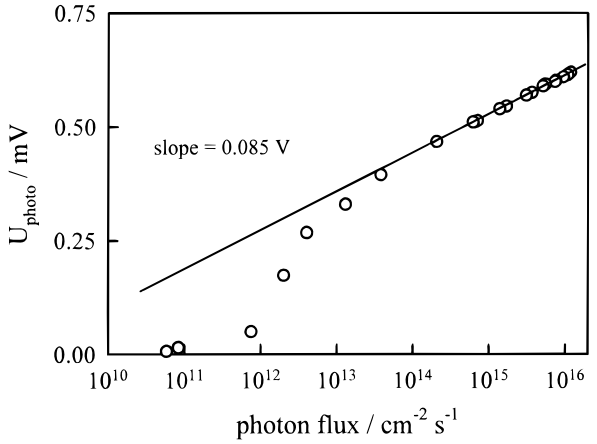

Figure 8. Intensity dependence of the dc photovoltage shown as a plot of U_{photo} vs photon flux.

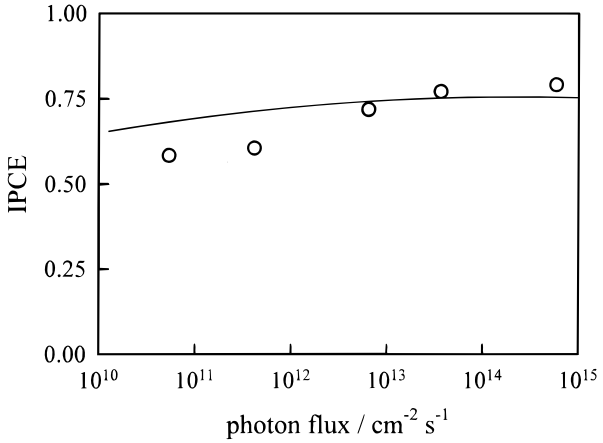

Figure 9. Comparison of experimental IPCE of cell (open circles) with the behavior predicted by fitting the IMPS and IMVS results (line).

which can be rewritten in the form

$$s(E_T) = \frac{N_{T0}}{k_B T_T} \exp\left[-\beta\left(\frac{E_c - E_T}{k_B T}\right)\right] \tag{17b}$$

where

$$\beta = \frac{T}{T_T} \tag{17c}$$

(normally the symbol α is used rather than β). T_T is a characteristic temperature that determines the broadening of the exponential distribution.

Evaluation of the ratio k_t/k_d for this distribution of traps shows that the variation of the effective diffusion coefficient with the electron QFL (and hence with the dc photovoltage) is given by

$$\frac{\partial \log D_n}{\partial U_{photo}} = (1-\beta)\frac{q}{2.303 k_B T} \tag{18}$$

This expression can be related to the observed dependence of D_n and U_{photo} on the incident dc photon flux as follows

$$\frac{\partial \log D_n}{\partial U_{photo}} = \frac{\partial \log D_n}{\partial \log I_0}\frac{1}{\dfrac{\partial U_{photo}}{\partial \log I_0}} \tag{19}$$

The intensity dependence of the photovoltage at open circuit gives a linear dependence of U_{photo} on the logarithm of the light intensity, although as Figure 8 shows, the photovoltage falls more steeply at low light intensities, possibly as the result of the finite internal shunt resistance of the cell. The slope of the plot of U_{photo} vs $\log(I_0)$ is 0.093 V, and the slope of the plot of $\log D_n$ vs $\log(I_0)$ is 0.68. β is therefore found from eqs 18 and 19 to be 0.57. Further work is required to establish how β (and consequently the intensity dependence of the IPCE) depends on oxide material and preparation methods.

The steady-state IPCE was measured directly (it is difficult to obtain reliable IPCE values of the DSNC at low intensities, since the photocurrent can take minutes to reach its steady-state value because τ_n is so long). The experimental IPCE was also obtained during the IMPS fitting as the low-frequency limit of the normalized photocurrent response. The experimental results are compared with the calculated IPCE in Figure 9. It can be seen that the calculated IPCE plot agrees quite well with the experimental values despite the difficulties of measuring the IPCE at low intensities. The agreement between the experimental values of the IPCE and those calculated from D_n and τ_n demonstrates the consistency of the approach adopted in this work.

The serendipitous compensation effects that give rise to the weak intensity dependence of the IPCE in the conventional Grätzel cell are unlikely to be encountered in systems in which the back reaction is first order in electron density. In these cases, the slowing of diffusion by trapping effects at low light intensities would not be compensated by an increase in electron lifetime because τ_n should be independent of n in the first-order case. Consequently, L_n (and hence the IPCE) should fall with decreasing intensity. The observation that the IPCE is almost independent of intensity in the conventional cell therefore provides further evidence for the second-order mechanism.

Conclusions

The present work has shown that the electron diffusion length of efficient DSNCs depends only weakly on light intensity because D_n and τ_n vary with light intensity in opposite senses. The intensity dependence of the electron lifetime is consistent with a second-order mechanism for the back reaction involving formation of $I_2^{\bullet-}$ as an intermediate. The intensity dependence of D_n is attributed to the effect of trapping/detrapping. The results suggest that attempts to replace the iodide/triiodide couple by simple one-electron redox systems are unlikely to be successful. In this case the kinetics of the back reaction should be first order in n, and τ_n is therefore independent of light intensity. This would mean that compensation for slow electron transport by slow back reaction is no longer possible.

Acknowledgment. This work was supported by the U.K. Engineering and Physical Sciences Research Council (EPSRC). L.M.P. acknowledges support from the Leverhulme Trust. The authors thank Juan Bisquert and Noel Duffy for helpful discussions and Ingo Uhlendorf (the Institut fur Angewandte Photovoltaik, Gelsenkirchen) for supplying electrolyte materials.

Appendix

Solutions of the Continuity Equations for First- and Second-Order Back Reaction. For illumination from the substrate side the general solution for the electron density is of the form[6]

$$\delta n(x,t) = u(x)\, e^{i\omega t} \tag{A1}$$

where

$$u(x) = A\,e^{\gamma x} + B\,e^{-\gamma x} + C\,e^{-\alpha x} \quad \text{(A2a)}$$

$$C = \frac{\alpha\,\delta I_0/D}{\gamma^2 - \alpha^2} \quad \text{(A2b)}$$

$$A = C\,\frac{\alpha\,e^{-\alpha d}(k_{ext} + \gamma D_n) - \gamma\,e^{-\gamma d}(k_{ext} + \alpha D_n)}{\gamma(k_{ext}(e^{\gamma d} + e^{-\gamma d}) + D_n\gamma(e^{\gamma d} - e^{-\gamma d}))} \quad \text{(A2c)}$$

$$B = -C\,\frac{\alpha\,e^{-\alpha d}(k_{ext} - \gamma D_n) + \gamma\,e^{\gamma d}(k_{ext} + \alpha D_n)}{\gamma(k_{ext}(e^{\gamma d} + e^{-\gamma d}) + D_n\gamma(e^{\gamma d} - e^{-\gamma d}))} \quad \text{(A2d)}$$

and

$$\gamma = \sqrt{\frac{1}{D_n\tau_n} + i\frac{\omega}{D_n}} \quad \text{(A2e)}$$

The solution for open-circuit conditions is obtained by setting $k_{ext} = 0$. The short-circuit solution is obtained by allowing k_{ext} to be large. The dc solutions are obtained by setting $\omega = 0$.

The frequency-dependent modulation of electron density at $x = 0$ is characterized by a semicircle in the lower complex plane with a minimum at $\omega = 1/\tau_n$. The IMVS response reflects the modulation of the electron QFL, and it is also a semicircle with $\omega_{min} = 1/\tau_n$.

The general expression for the normalized photocurrent is obtained from eqs A2a and A4

$$\frac{j_{photo}}{\delta I_0} = D(\gamma A - \gamma B - \alpha C) \quad \text{(A3)}$$

The limiting expression for diffusion-controlled extraction is obtained by allowing k_{ext} to be infinite in the above expression. In practice for $D_n = 10^{-5}$ cm^2 s^{-1}, the diffusion-limited case is obtained for $k_{ext} > 1$ cm s^{-1}. The steady-state solution is obtained by setting $\omega = 0$.

In the case of second-order back reaction of electrons with I_3^-, the continuity equation is

$$\frac{dn}{dt} = \eta\alpha I_0\,e^{-\alpha x} + D_n\frac{d^2n}{dx^2} - k(n - n_0)^2 \quad \text{(A4)}$$

The boundary conditions are the same as those used in the case of eq A1. Equation A4 was solved numerically by the fully implicit finite difference method[29] to give the steady-state electron density profiles and the steady-state photocurrents.

The small-amplitude solution of the second-order case is obtained by noting that expansion and linearization of the time dependence of the excess electron concentration lead to definition of the electron lifetime as $\tau_n = 1/(kn)$. Equations A2 and A3 can then be used to obtain the corresponding IMVS and IMPS responses.

Influence of Electron Trapping on the IMPS Response. For a set of electron traps located at a given energy, the solution of the continuity equation takes the same form as above except that the γ term includes the effects of trapping, detrapping, and back reaction via the conduction band and via surface states:[6]

$$\gamma^2 = \left(\frac{1}{D_{cb}\tau_{cb}}\right) + \frac{k_t}{D_{cb}}\frac{\frac{1}{\tau_t}\left(k_d + \frac{1}{\tau_t}\right) + \omega^2}{\left(k_d + \frac{1}{\tau_t}\right)^2 + \omega^2} + i\frac{\omega}{D}\left[1 + \frac{k_t k_d}{\left(k_d + \frac{1}{\tau_t}\right)^2 + \omega^2}\right] \quad \text{(A5)}$$

The first-order trapping rate constant k_t (s^{-1}) is determined by the thermal velocity of electrons in the conduction band (υ_{th}), the number density of vacant traps, $N_t(1 - f_t)$, and their capture cross section σ_t: $k_t = \sigma\upsilon N_t(1 - f_t)$. The thermal detrapping rate constant k_d depends exponentially on the trap depth (optical detrappping is neglected in this model). Both free and trapped electrons may back-react with I_3^-; these processes are described by the lifetimes τ_{cb} and τ_t, respectively. In the case of a distribution of traps, the trap density at the quasi-Fermi level determines k_t, and the position of the QFL relative to the conduction band determines k_d. An exact treatment of this problem will be given elsewhere.[23]

If the trapping and detrapping processes are fast on the time scale of the modulation and $k_t \gg k_d$, eq A5 reduces to the expression for the trap-free case with the electron lifetime given by τ_t and an effective diffusion coefficient $D_n = D_{cb}(k_d/k_t)$. It follows that analysis of the IMPS response gives D_n to a good approximation, whereas IMVS gives τ_t.

References and Notes

(1) O'Regan, B.; Grätzel, M. *Nature* **1991**, *353*, 737.

(2) Vlachopoulos, N.; Liska, P.; Augustysnski, J.; Grätzel, M. *J. Am. Chem. Soc.* **1988**, *110*, 1216.

(3) Nazeeruddin, M.; Kay, A.; Rodicio, I.; Humphry-Baker, R.; Mueller, E.; Liska, P.; Vlachopoulos, N.; Grätzel, M. *J. Am. Chem. Soc.* **1993**, *115*, 6382.

(4) Södergren, S.; Hagfeldt, A.; Olsson, J.; Lindquist, S. E. *J. Phys. Chem.* **1994**, *95*, 5522.

(5) Cao, F.; Oskam, G.; Meyer, G. J.; Searson, P. C. *J. Phys. Chem.* **1996**, *100*, 17021.

(6) Dlocik, L.; Ileperuma, O.; Lauermann, I.; Peter, L. M.; Ponomarev, E. A.; Redmond, G. *J. Phys. Chem. B* **1997**, *101*, 10281.

(7) Peter, L. M.; Vanmaekelbergh, D. *Advances in Electrochemical Science and Engineering*; Alkire, R. C., Kolb, D. M., Eds.; Wiley-Interscience: Chichester, U.K., 1999; Vol. 6, p 77.

(8) Fitzmaurice, D. J.; Frei, H. *Langmuir* **1991**, *7*, 1120.

(9) Nasr, C.; Hotchandani, S.; Kamat, P. V. *J. Phys. Chem. B* **1998**, *102*, 4944.

(10) O'Regan, B.; Moser, J.; Anderson, M.; Grätzel, M. *J. Phys. Chem.* **1990**, *94*, 8720.

(11) Haque, S. A.; Tachibana, Y.; Klug, D. R.; Durrant, J. R. *J. Phys. Chem. B* **1998**, *102*, 1745.

(12) Franco, G.; Gehring, J.; Peter, L. M.; Ponomarev, E. A.; Uhlendorf, I. *J. Phys. Chem.* **1999**, *103*, 692.

(13) Peter, L. M.; Shaw, N. J. Unpublished results.

(14) Huang, S. Y.; Schlichthörl, G.; Nozik, A. J.; Grätzel, M.; Frank, A. J. *J. Phys. Chem. B* **1997**, *101*, 2576.

(15) Schlichthörl, G.; Huang, S. Y.; Sprague, J.; Frank, A. J. *J. Phys. Chem. B* **1997**, *101*, 8141.

(16) Schlichthörl, G.; Park, N. G.; Frank, A. J. *J. Phys. Chem. B* **1999**, *103*, 782.

(17) Nelson, I. V.; Iwamoto, R. T. *J. Electroanal. Chem.* **1964**, *7*, 218.

(18) Vanmaekelbergh, D.; de Jongh, P. E. *J. Phys. Chem. B* **1999**, *103*, 747.

(19) Forro, L.; Chauvet, O.; Emin, D.; Zuppiroli, L.; Berger, H.; Lévy, F. *J. Appl. Phys.* **1994**, *75*, 633.

(20) Marshall, J. M. *Rep. Prog. Phys.* **1983**, *46*, 1235.
(21) Nelson, J. *Phys. Rev. B* **1999**, *59*, 15374.
(22) Vanmaekelbergh, D.; de Jongh, P. E. Manuscript submitted.
(23) Peter, L. M.; Walker, A. B. Manuscript in preparation.
(24) Bisquert, J.; Garcia-Belmonte, G.; Fabregat-Domingo, F. *J. Solid State Electrochem.* **1999**, *3*, 337.
(25) Schwarzburg, K.; Willig, F. *J. Phys. Chem. B* **1999**, *103*, 5743.
(26) Peter, L. M.; Ponomarev, E. A.; Franco, G.; Shaw, N. J. *Electrochim. Acta* **1999**, *45*, 549.
(27) Liu, Y.; Hagfeldt, A.; Xiao, X. R.; Lindquist, S. E. *Sol. Energy Mater. Sol. Cells* **1998**, *55*, 267.
(28) Fitzmaurice, D. J.; Eschle, M.; Frei, H.; Mosser, J. *J. Phys Chem.* **1993**, *97*, 3806.
(29) Fisher, A. C.; Compton, R. G. *J. Phys. Chem.* **1986**, *90*, 247.